High-Resolution Double-Quantum ^{31}P MAS NMR Study of the Intermediate-Range Order in Crystalline and Glass Lead Phosphates

Franck Fayon,* Catherine Bessada, Jean-Pierre Coutures, and Dominique Massiot

Centre de Recherche sur les Matériaux à Hautes Températures, CNRS,
1D Avenue de la Recherche Scientifique, 45071 Orléans Cedex 2, France

Received April 6, 1999

We have investigated the structure of binary lead phosphate glasses using 1D ^{31}P MAS and 2D ^{31}P double-quantum NMR. The distribution of the Q_n phosphate species, determined from the simulation of 1D MAS spectra, indicates a significant disproportionation reaction ($2Q_n \leftrightarrow Q_{n+1} + Q_{n-1}$) near the pyrophosphate composition. As demonstrated on crystalline reference samples, 2D double-quantum experiments can be used to determine the connectivities between Q_n groups. This allows us to probe the phosphorus connectivity scheme in the glass network and to show that the Q_n chemical shift is influenced by the type of the bonded PO_4 tetrahedron. By analyzing quantitative 1D MAS spectra and 2D double-quantum spectra, we have determined the phosphorus connectivity scheme in the glass structure and its evolution with composition.

Introduction

Recently, a whole range of new applications of phosphate-based glasses have been developed[1,2] (laser glasses, optoelectronics, nuclear waste storage). A clear characterization and understanding of their structure on different length scales is thus highly desirable but remains experimentally difficult, mainly due to their lack of periodicity. Different techniques such as Raman scattering, XPS, IR and NMR spectroscopies have already been used to study the local ordering around phosphorus.[3] In phosphate glasses, phosphorus always occurs in tetrahedral coordination. The different tetrahedra can be classified according to their connectivities, Q_n, where n represents the number of bridging oxygen atoms per PO_4 tetrahedron ($n = 0-3$). However, the description of the intermediate range order in these systems, i.e., the ordering of basic structural units within the second and third coordination spheres of the phosphorus atoms, still remains a question. Solid-state nuclear magnetic resonance (NMR) spectroscopy has proved to be a powerful tool for the structural analysis of disordered solids such as glasses.[4] In particular, the different Q_n units constituting the phosphate network have been clearly evidenced in high-resolution magic angle spinning (MAS) NMR spectra through the ^{31}P chemical shift interaction which is sensitive to the phosphorus local environment. Furthermore, the through-space magnetic dipolar interaction strongly depends on the inter-nuclei distance and can be used to probe the spatial connectivity between atoms in solids. This interaction is averaged out under fast MAS spinning required for obtaining high-resolution spectra. In the case of spin $^1/_2$ nuclei like ^{31}P, several pulse sequences have been developed to selectively reintroduce the homonuclear dipolar interaction in rotating solids.[5−11] This allows one to obtain a MAS-resolved spectrum that provides both the chemical shift and the homonuclear dipolar information. These sequences, designed for two-dimensional magnetization exchange experiments or double-quantum NMR spectroscopy, have been recently employed with success to characterize the phosphorus connectivity scheme in crystalline phosphates[12,13] and glasses.[14−18]

In the case of the binary lead phosphate glasses, the local lead environment has previously been probed by EXAFS,[19] X-ray diffraction,[20] and ^{207}Pb NMR.[21] However, the structure of the phosphate network has not been thoroughly investigated. In this work, we used ^{31}P one-dimensional MAS and two-dimensional double-quantum NMR to study the short and intermediate range structure of crystalline phases and glasses in the binary xPbO$(1-x)$P$_2$O$_5$ system with x varying from 0.5 to 0.67.

(1) Weber, M. J. *J. Non-Cryst. Solids* **1990**, *123*, 208−222.
(2) Sales, B. C.; Boatner, L. A. *Science* **1984**, *226*, 45−48.
(3) Martin, S. W. *Eur. J. Solid State Inorg. Chem.* **1991**, *28*, 163−205.
(4) Eckert, H. *Prog. Nucl. Magn. Reson. Spectrosc.* **1992**, *24*, 159−293.
(5) Tycko, R.; Dabbagh, G. *J. Am. Chem. Soc.* **1991**, *113*, 9444−9448.
(6) Bennett, A. E.; Ok, J. H.; Griffin, R. G.; Vega, S. *J. Chem. Phys.* **1992**, *96*, 8624−8627.
(7) Nielsen, N. C.; Bildsøe, H.; Jakobsen, H. J.; Levitt, M. H. *J. Chem. Phys.* **1994**, *101*, 1806−1812.
(8) Sun, B. Q.; Costa, P. R.; Kocisko, D.; Lansbury, P. T.; Griffin, R. G. *J. Chem. Phys.* **1995**, *102*, 702−707.
(9) Baldus, M.; Tomaselli, M.; Meier, B. H.; Ernst, R. R. *Chem. Phys. Lett.* **1994**, *230*, 329−336.
(10) Lee, Y. K.; Kurur, N. D.; Elm, M.; Johannessen, O. G.; Nielsen, N. C.; Levitt, M. H. *Chem. Phys. Lett.* **1995**, *242*, 304−309.
(11) Feike, M.; Demco, D. E.; Graf, R.; Gottwald, J.; Hafner, S.; Spiess, H. W. *J. Magn. Reson. A* **1996**, *122*, 214−221.
(12) Feike, M.; Graf, R.; Schnell, I.; Jäger, C.; Spiess, H. W. *J. Am. Chem. Soc.* **1996**, *118*, 9631−9634.
(13) Geen, H.; Gottwald, J.; Graf, R.; Schnell, I.; Spiess, H. W.; Titman, J. J. *J. Magn. Reson.* **1997**, *125*, 224−227.
(14) Jäger, C.; Feike, M.; Born, R.; Spiess, H. W. *J. Non-Cryst. Solids* **1994**, *180*, 91−95.
(15) Olsen, K. K.; Zwanziger, J. W.; Hartmann, P.; Jäger, C. *J. Non-Cryst. Solids* **1997**, *222*, 199−205.
(16) Alam, T. M.; Brow, R. K. *J. Non-Cryst. Solids* **1998**, *223*, 1−20.
(17) Feike, M.; Jäger, C.; Spiess, H. W. *J. Non-Cryst. Solids* **1998**, *223*, 200−206.
(18) Witter, R.; Hartmann, P.; Vogel, J.; Jäger, C. *Solid State NMR* **1998**, *13*, 189−200.
(19) Greaves, G. N.; Gurman, S. J.; Gladden, L. F.; Spence, C. A.; Cox, P.; Sales, B. C.; Boatner, L. A.; Jenkins, R. N. *Philos. Mag.* **1988**, *B58*, 271−283.
(20) Lai, A.; Musinu, A.; Piccaluga, G.; Puligheddu, S. *Phys. Chem. Glasses* **1997**, *38*, 173−178.
(21) Fayon, F.; Bessada, C.; Douy, A.; Massiot, D. *J. Magn. Reson.* **1999**, *137*, 116−121.

10.1021/ic990375p CCC: $18.00
Published on Web 10/21/1999

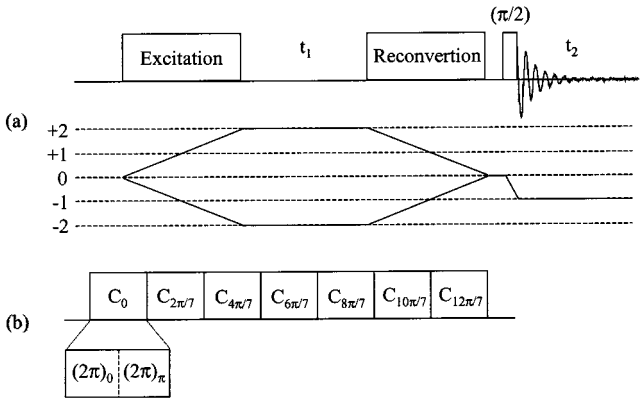

Figure 1. (a) Pulse sequence and coherence pathway used for the two-dimensional double-quantum MAS experiments. (b) Detail of the C7 sequence used for double-quantum excitation and reconversion. It involves seven phase-shifted pulse cycles timed to span two rotor periods, each cycle consisting of two (2π) pulses with opposed phases.[10]

Experimental Section

The P_2O_5-PbO glasses were prepared from reagent grade PbO and $(NH_4)_2HPO_4$. The glass samples were melted in Pt crucibles for 1h in an electric furnace under air at temperature varying from 700 to 850 °C depending on composition and quenched by partly immersing the crucible in water. An additional 0.02 mol % of Fe_2O_3 was included in the batch to reduce the ^{31}P relaxation time. Glass compositions were checked by microprobe (1 mol % uncertainties). The $Pb_2P_2O_7$, $Pb_3P_4O_{13}$, and $Pb(PO_3)_2$ crystalline phases were obtained by annealing the glasses at high temperature and checked by powder X-ray diffraction.

The solid-state NMR experiments were performed on a Bruker DSX 300 spectrometer with a 4 mm MAS probehead operating at a Larmor frequency of 121.4 MHz for ^{31}P. The $\pi/2$ pulse duration was 3.5 μs ($\omega_{rf}/2\pi = 71.4$ kHz). The one-dimensional (1D) ^{31}P MAS spectra were recorded at 3 and 10 kHz spinning rates using single pulse ($\pi/12$) acquisition with recycle delay varying from 2 to 20 s to ensure no saturation.

The two-dimensional (2D) ^{31}P double-quantum NMR spectra were acquired while spinning at 10 kHz using the pulse sequence depicted in Figure 1. The aim of this experiment is to correlate the usual 1D MAS spectrum, characteristic of the individual ^{31}P resonances, to the double-quantum spectrum, characteristic of the resonance of pairs of nearby ^{31}P atoms coupled by dipolar interaction. The initial excitation period is used to create the double-quantum coherence which is allowed to evolve during an incremented time t_1. During the reconversion period, the double-quantum coherence is reconverted to Zeeman magnetization and the final $\pi/2$ pulse is applied to create transverse magnetization acquired during the detection time t_2 (FID). The t_1 modulated signal acquired during t_2 is then doubly Fourier transformed (according to t_1 and t_2 times) to obtain a two-dimensional correlation spectrum that correlates a double-quantum spectrum to a "double-quantum filtered" single-quantum MAS spectrum. A pair of coupled nuclei, which resonate individually at frequencies ω_A and ω_B in the single-quantum ω_2 dimension, resonate at the sum of the frequencies ($\omega_A + \omega_B$) in the double-quantum ω_1 dimension. Consequently, double-quantum coherence involving two distinct sites is evidenced by twin cross-correlation peaks on each side of the diagonal of the two-dimensional spectrum, while double-quantum coherence between two equivalent sites gives a single autocorrelation peak on the diagonal. Since the homonuclear dipolar interaction is averaged out by magic angle spinning, a recoupling sequence has to be used to create a dipolar double-quantum Hamiltonian. We have used the C7 recoupling sequence[10] to achieve an efficient broadband excitation and reconversion of double-quantum coherences under MAS conditions ($\omega_{rf}/2\pi = 69.5$ kHz at a spinning rate of 10 kHz). The excitation and reconversion periods were kept short (600 μs), and under these conditions, the intensity of double-quantum resonances is proportional to the square of the dipolar coupling and to the number of coupled spin pairs.[22] The phases of the C7 excitation sequence and of the last $\pi/2$ pulse were cycled by step of 90° to select the coherence pathway of Figure 1. The two-dimensional pure absorption phase spectra were obtained using a hypercomplex acquisition.[23] Processing of the 2D spectra was made using the RMN program.[24] To avoid spinning sidebands in the ω_1 dimension, the t_1 time increment was synchronized with the rotor period; 128 and 64 t_1 increments were taken for the crystalline and glass samples, respectively. Each slice was the sum of 16 transients using a recycle delay of 20 s. The entire experimental time required to acquire the 2D spectrum was about 12 and 6 h for the crystalline and glass samples, respectively. The spinning frequency was stabilized to ±10 Hz for all experiments. ^{31}P chemical shifts were referenced relative to 85% H_3PO_4 solution at 0 ppm.

Table 1. Isotropic and Anisotropic ^{31}P Chemical Shifts of the Crystalline Lead Phosphates $Pb_2P_2O_7$, $Pb_3P_4O_{13}$, and $Pb(PO_3)_2$ (δ_{ISO} ± 0.5 ppm, Ω ± 2 ppm, K ± 0.02) with $\Omega = \delta_{11} - \delta_{33}$, $K = 3(\delta_{22} - \delta_{iso})/\Omega$[36]

compound	δ_{ISO} (ppm)	Ω (ppm)	K	δ_{11} (ppm)	δ_{22} (ppm)	δ_{33} (ppm)
$Pb_2P_2O_7$ A	−8.4	133.2	−0.69	73.6	−39.2	−59.6
B	−8.9	130	−0.69	71.1	−38.9	−58.9
C	−11.3	140.2	−0.38	67.7	−29.1	−72.5
D	−12	142	−0.38	68	−30	−74
$Pb_3P_4O_{13}$ E	−9.9	147.3	−0.38	73.1	−28.6	−74.2
F	−10.8	158.4	−0.33	77.2	−28.4	−81.2
G	−23.9	209.4	0.38	67.2	2.6	−141.9
H	−25.3	201.6	0.33	64.3	−2.9	−137.3
$Pb(PO_3)_2$ I	−27.8	207.7	0.38	62.9	−1.5	−144.8
J	−28.7	204.1	0.38	60.4	−2.8	−143.7
K	−30.5	224	0.43	65.5	1.5	−158.5
L	−31.8	216.5	0.38	62.75	−4.35	−153.8

Results and Discussion

Crystalline Lead Phosphates. To carry out a comprehensive interpretation of spectra obtained on glasses, we have first studied crystalline reference compounds of known structure, for which new methods can be validated. Preliminary 1D ^{31}P NMR results have been reported for $Pb_2P_2O_7$ and $Pb(PO_3)_2$.[25] We shall first report our results obtained for $Pb_2P_2O_7$, $Pb_3P_4O_{13}$, and $Pb(PO_3)_2$ using ^{31}P MAS NMR and two-dimensional ^{31}P double-quantum NMR.

The high spinning rate ^{31}P MAS spectra (10 kHz) of the reference samples $Pb_2P_2O_7$, $Pb_3P_4O_{13}$, and $Pb(PO_3)_2$ (not shown) exhibit resolved sharp lines from which isotropic chemical shifts can be easily measured. These crystalline lead phosphates give examples of Q_1 and Q_2 phosphorus sites with isotropic shifts in the ranges −8, −12 ppm and −23, −32 ppm, respectively. These values are in agreement with the ^{31}P chemical shift trends described in the literature.[3] The chemical shift anisotropy (CSA) tensors of the ^{31}P crystalline sites were determined from the spinning sideband intensities in MAS spectra[26] with sample spinning at 3 kHz, neglecting the residual dipolar interaction. The experimental slow spinning ^{31}P MAS spectra and their simulations, according to the parameters given in Table 1, are presented in Figure 2. It can be noticed that the distinction between Q_1 and Q_2 resonances can also be made on the basis

(22) Gottwald, J.; Demco, D. E.; Graf, R.; Spiess, H. W. *Chem. Phys. Lett.* **1995**, *243*, 314−323.
(23) Ernst, R. R.; Bodenhausen, G.; Wokaun, A. *Principles of Nuclear Magnetic Resonance in One and Two Dimensions*; Clarendon Press: Oxford, 1987.
(24) Grandinetti, P. J. *RMN*, v1.2.1; Department of Chemistry, The Ohio State University, Columbus, OH 43210-1173 USA (http://chemistry.ohio-state.edu/~grandinetti/RMN).
(25) Prabhakar, S.; Rao, K. J.; Rao, C. N. R. *Chem. Phys. Lett.* **1987**, *139*, 96−102.
(26) Herzfeld, J.; Berger, A. E. *J. Chem. Phys.* **1980**, *73*, 6021−6030.

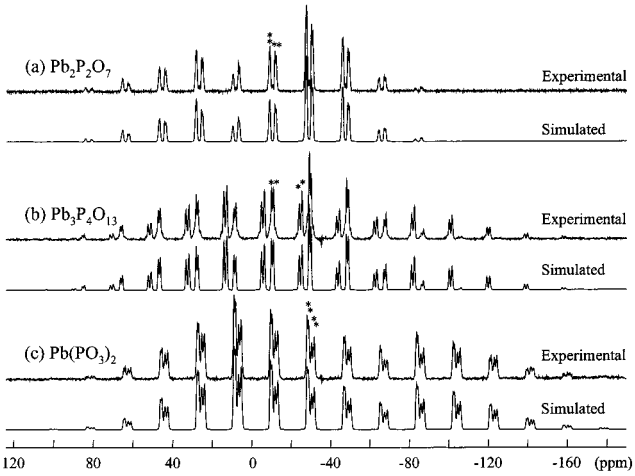

Figure 2. ^{31}P MAS NMR spectra (3 kHz spinning rate) of $Pb_2P_2O_7$, $Pb_3P_4O_{13}$, and $Pb(PO_3)_2$. The asterisks mark isotropic peaks.

of their chemical shift anisotropies (sign of the skew parameter (K) and span of the chemical shift anisotropy).

The structure of the lead pyrophosphate $Pb_2P_2O_7$ contains four crystallographically inequivalent Q_1 units linked together to form two $[P_2O_7]^{4-}$ anions.[27] The 1D MAS NMR spectrum shown in Figure 2 evidences four isotropic peaks, A, B, C, and D at −8.4, −8.9, −11.3, and −12 ppm, respectively, that correspond to the four Q_1 sites present in the structure. The 2D double-quantum spectrum of $Pb_2P_2O_7$ is displayed in Figure 3a. This spectrum exhibits two intense cross-correlation peaks (A−C) and (B−D) that indicate dipolar connectivity between the two inequivalent Q_1 sites of $[P_2O_7]^{4-}$ groups. In addition, four weak autocorrelation peaks appear on the diagonal of the double-quantum spectrum and reflect the spatial proximity of the equivalent $[P_2O_7]^{4-}$ anions. The intensity ratio between cross and autocorrelation peaks is about 4:1. In the $Pb_2P_2O_7$ structure, the internuclear P−P distances between chemically linked Q_1 units (P−O−P bond) are approximately 0.3 nm and are significantly shorter than the other next nearest P−P distances that exceed 0.4 nm, since dipolar interaction varies as $1/r^3$. This allows to differentiate dipolar coupling between chemically linked PO_4 groups and weaker long-range dipolar interaction in the double-quantum spectrum and thus to identify clearly the P−O−P connectivity scheme.

The structure of the lead tetrapolyphosphate $Pb_3P_4O_{13}$ is made of two inequivalent Q_1 units and two inequivalent Q_2 units associated together to form a linear $[P_4O_{13}]^{6-}$ anion.[28] The MAS NMR spectrum shown in Figure 2 clearly exhibits four distinct contributions in agreement with the structure. The two isotropic peaks at −9.9 and −10.8 ppm, labeled E and F, respectively, are attributed to the two Q_1 sites and the two isotropic peaks at −23.9 and −25.3 ppm, labeled G and H, respectively, correspond to the Q_2 resonances. The double-quantum spectrum of $Pb_3P_4O_{13}$ presented in Figure 3b shows three intense cross-correlation peaks E−G, F−H, and G−H, that reflect the dipolar connectivity between chemically bound PO_4 tetrahedra. The weaker autocorrelation peaks observed on the double-quantum diagonal correspond to weaker dipolar coupling between nearby but not linked equivalent Q_n groups. This double-quantum spectrum thus evidences a connectivity scheme E−G−H−F and is characteristic of a linear tetrameric $[P_4O_{13}]^{6-}$ anion.

The structure of the lead metaphosphate $Pb(PO_3)_2$ consists of infinite phosphate chains containing four inequivalent PO_4 tetrahedra.[29] Four isotropic resonances at −27.8, −28.7, −30.5, and −31.8 ppm, labeled I, J, K, and L, respectively, are displayed in the MAS NMR spectrum (Figure 2) and correspond to these four distinct Q_2 sites. The double-quantum spectrum of $Pb(PO_3)_2$ is shown in Figure 3c. In this case, the small difference between the coupled spin pairs resonances lead to an unresolved spectrum in the double-quantum dimension. However, the correlation peaks can be determined by carefully analyzing separated 1D slices of the 2D double-quantum experiment. Following this analysis, the 2D spectrum indicates connectivities between resonances I−K, J−K, I−L, and J−L. In analogy with $Pb_2P_2O_7$ and $Pb_3P_4O_{13}$, the weaker diagonal autocorrelation intensities illustrate the spatial proximity of non-chemically bound PO_4 groups. This spectrum is thus characteristic of a linear or cyclic phosphate chain with four inequivalent Q_2 sites per period.

From the study of these crystalline compounds and on the basis of their known structures,[27−29] we clearly show that the high-resolution double-quantum/single-quantum homonuclear dipolar correlation spectroscopy can be used to selectively probe the P−O−P connectivity scheme of crystalline or amorphous phosphate networks.

Lead Phosphate Glasses. As expected, the MAS NMR spectra of ^{31}P in the glasses are less resolved than those of the crystalline samples. Figure 4 shows the evolution of the ^{31}P 1D MAS NMR spectra (10 kHz) of the $PbO-P_2O_5$ glasses as a function of the lead content from 67 to 50 mol % PbO. These spectra exhibit partly overlapping isotropic resonances with their associated spinning sidebands due to an incomplete averaging of the CSA interaction under magic angle spinning. These three distinct isotropic contributions can be assigned to Q_2, Q_1, and Q_0 units according to the ^{31}P chemical shift ranges in crystalline lead phosphates. In agreement with previous works,[25] the MAS spectrum of the metaphosphate glass is dominated by an intense isotropic peak at about −24 ppm that correspond to Q_2 units involved in long phosphate chains or cycles. As the PbO content increases, the intensity of the Q_1 resonance, centered at about −9 ppm, increases indicating a progressive depolymerization of the phosphate network. The last isotropic component at 1.5 ppm is attributed to the Q_0 units, in analogy with the ^{31}P isotropic shift of the $[PO_4]^{3-}$ group in $Pb_3(PO_4)_2$ ($\delta_{ISO} = -0.2$ ppm).

The experimental 1D MAS spectra can be satisfactorily simulated (including spinning sidebands) under simple hypothesis, i.e., assuming Gaussian line shapes for each Q_n unit. For the metaphosphate glass, a low Q_3 intensity at −38 ppm was taken in account in our simulation. From these simulations, the relative Q_n site populations were obtained for each glass composition. Table 2 gives the isotropic chemical shifts, line widths, and relative Q_n concentrations for the different samples. Figure 5 shows the evolution of the experimentally determined Q_n populations from which we have calculated the equilibrium constants k_n of the disproportionation reactions:[30,31]

$$2Q_n \leftrightarrow Q_{n+1} + Q_{n-1}$$

The obtained equilibrium constants are $k_2 = 0.001 \pm 0.002$ and $k_1 = 0.022 \pm 0.013$. For the glasses having a PbO content

(27) Mullica, D. F.; Perkins, H. O.; Grossie, D. A.; Boatner, L. A.; Sales, B. C. *J. Solid State Chem.* **1986**, *62*, 371−376.
(28) Averbuch-Pouchot, T.; Durif, A. *Acta Crystallogr.* **1987**, *C43*, 631−632.
(29) Jost, K. H. *Acta Crystallogr.* **1964**, *17*, 1539−1544.
(30) Parks, J. R.; Van Wazer, J. R. *J. Am. Ceram. Soc.* **1957**, *79*, 4890−4897.
(31) Stebbins, J. F. *Nature* **1987**, *330*, 465−467.

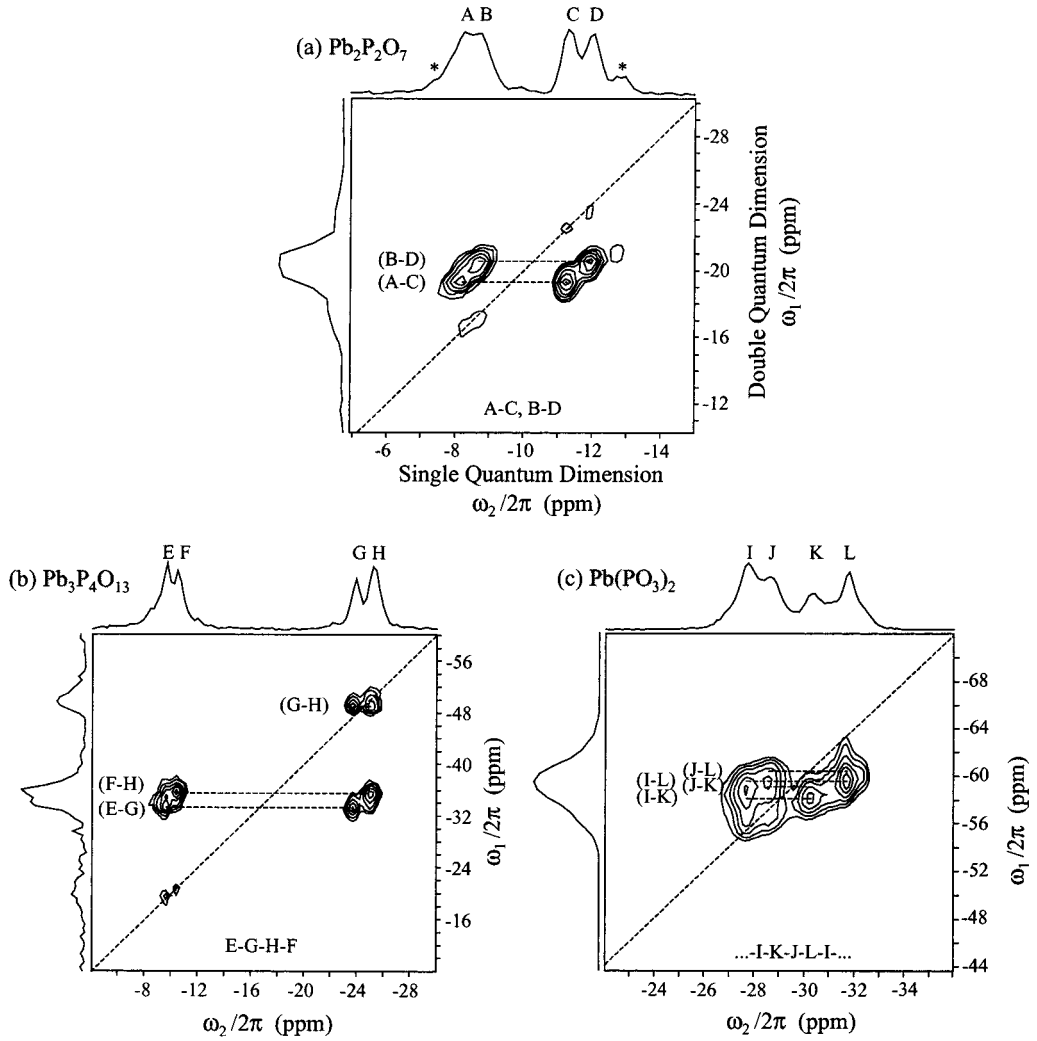

Figure 3. High-resolution ^{31}P double-quantum MAS spectra of $Pb_2P_2O_7$ (a), $Pb_3P_4O_{13}$ (b), and $Pb(PO_3)_2$ (c). The contour levels were set to 14.8, 20.8, 29.1, 40.8, 57.1, and 80% of the maximal peak intensity. Asterisks mark impurities.

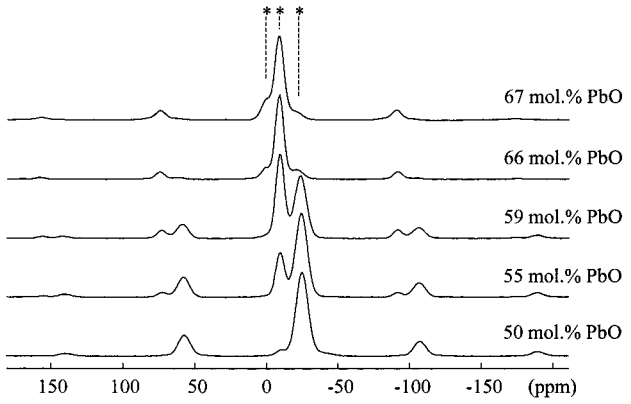

Figure 4. ^{31}P MAS NMR spectra (10 kHz spinning rate) of the lead phosphate glasses. The asterisks mark isotropic peaks.

close to 50 mol %, the Q_n distribution is close to a binary distribution ($k_2 \approx 0$) as expected for an ionic modifier cation.[30] However, the equilibrium constant calculated for the disproportionation reaction of Q_1 species indicates a more random configuration of bridging and non bridging oxygen atoms as the lead content increases. This evolution can be attributed to the appearance of more covalent Pb−O bonds in the glass structure, in full agreement with our interpretation of two-dimensional ^{207}Pb PASS NMR spectra that evidence the mixed network former/network modifier role of Pb^{2+} in P_2O_5−PbO glasses with high lead content.[21] It should be noticed that these equilibrium constants are very similar to those determined in zinc phosphate glasses[32] and are 1 order of magnitude weaker than those measured in lead silicate glasses.[33]

Table 2. Isotropic ^{31}P Chemical Shifts (δ_{ISO}), Line Widths (Full Width at Half-Maximum, fwhm), and Relative Intensities (I%) of the Q_n Units in the PbO−P_2O_5 Glasses ($\delta_{ISO} \pm 0.2$ ppm, fwhm $\pm$ 0.5 ppm, $I \pm 5\%$)

	Q_3	Q_2	Q_1	Q_0
mol % PbO	δ_{ISO} (fwhm) I	δ_{ISO} (fwhm) I	δ_{ISO} (fwhm) I	δ_{ISO} (fwhm) I
50	−38.3 (13.2) 3.5	−24.6 (9.9) 93.7	−9.7 (7.1) 2.8	−
55	−	−24.0 (9.8) 74.5	−9.2 (7.3) 25.5	−
59	−	−23.2 (9.8) 54.4	−8.9 (7.2) 44.6	1.5 (7.1) 1.0
66	−	−20.5 (10.0) 13.9	−8.3 (7.0) 77.1	1.5 (7.1) 9.0
67	−	−20.1 (10.0) 9.9	−8.0 (7.8) 75.8	1.5 (7.2) 14.3

For each type of Q_n unit present in the glass, the line width is related to a continuous distribution of isotropic chemical shift. This inhomogeneous broadening arises from structural disorder

(32) Brow, R. K.; Tallant, D. R.; Myers, S. T.; Phipher, C. C. *J. Non-Cryst. Solids* **1995**, *191*, 45−55.
(33) Fayon, F.; Bessada, C.; Massiot, D.; Farnan, I.; Coutures, J. P. *J. Non-Cryst. Solids* **1998**, *232−234*, 403−408.

Table 3. Isotropic ^{31}P Chemical Shifts (δ_{ISO}), Line Widths (Full Width at Half-Maximum, fwhm), and Relative Intensities ($I \pm 7\%$) of the $Q_{n,ij}$ Units in the $PbO-P_2O_5$ Glasses

$Q_{n,ij}$ unit	Q_0	$Q_{1,1}$	$Q_{1,2}$	$Q_{2,11}$	$Q_{2,21}$	$Q_{2,22}$
δ_{ISO} (ppm)	1.5 ± 0.5	-8.0 ± 0.5	-9.5 ± 0.5	-20.0 ± 0.5	-22.5 ± 0.5	-24.5 ± 0.5
fwhm (ppm)	7.0 ± 0.5	7.0 ± 0.5	7.0 ± 0.5	8.5 ± 0.5	8.5 ± 0.5	9.0 ± 0.5
55 mol % PbO, intensity (%)	−	1.5	23.7	3.0	17.7	54.1
59 mol % PbO, intensity (%)	0.9	13.6	30.7	6.0	18.7	30.1
66 mol % PbO, intensity (%)	8.7	59.3	19.2	7.9	3.4	1.5
67 mol % PbO, intensity (%)	14.6	58.7	17.1	7.5	2.1	−

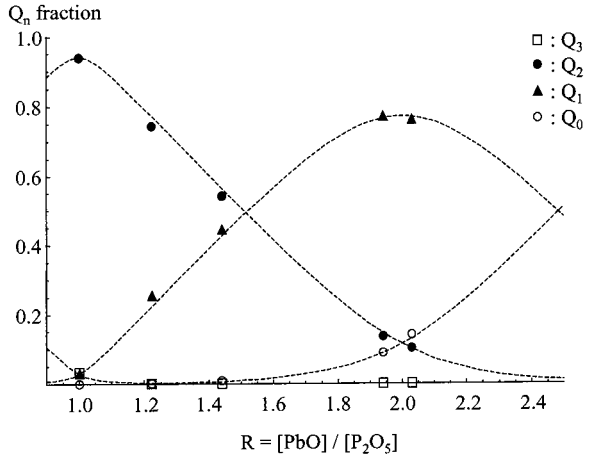

Figure 5. Experimentally determined Q_n distribution in lead phosphate glasses as a function of the $[PbO]/[P_2O_5]$ ratio. The fitted lines were calculated from the equilibrium constants $k_2 = 0.001$ and $k_1 = 0.022$.

such as bond angles, bond lengths variations and higher coordination sphere disorder. It should be noticed that the Q_n line width increases significantly with the number of bridging oxygen atoms per Q_n units (Table 2). As in the case of other phosphate glasses,[34,35] we can also remark that the individual Q_n isotropic shifts depend on glass composition. It increases linearly (^{31}P deshielding) with PbO content, with an increasing slope going from Q_0 to Q_2.

This description of the glass structure is limited to the short-range order. As shown for the crystalline samples, it is possible to selectively probe the dipolar couplings between chemically linked PO_4 tetrahedra using double-quantum NMR experiments. We can then describe the Q_n connectivity scheme and the intermediate range order of the glass network.

The 2D double-quantum spectra of the $PbO-P_2O_5$ glasses are presented in Figure 6. The double-quantum spectrum of the glass containing 66 mol % PbO (Figure 6a) is composed of Q_1-Q_2 cross-correlation peaks and an intense Q_1-Q_1 autocorrelation peak typical of a $[P_2O_7]^{4-}$ unit. No Q_2-Q_2 autocorrelation peak is evidenced in the spectrum. This indicates that the Q_2 species are mainly linked to two Q_1 units to form a $[P_3O_{10}]^{5-}$ group. We also remark that, as expected, the Q_0 resonance, which is present in the 1D MAS spectrum, is filtered out of the double-quantum spectrum. In this case, a qualitative analysis of both MAS and double-quantum spectra shows that the phosphate network is mostly constituted of $[P_2O_7]^{4-}$, $[PO_4]^{3-}$, and $[P_3O_{10}]^{5-}$ groups. This is in contrast with the $Pb_2P_2O_7$ crystalline structure (of same composition) that contains only $[P_2O_7]^{4-}$ anions.

The double-quantum spectrum of the glass containing 59 mol % PbO (Figure 6b) exhibits three separated correlation peaks. The two intense resonances, located at approximately −31 ppm and −48 ppm in the double-quantum dimension, correspond respectively to the Q_1-Q_2 and Q_2-Q_2 pairs that are involved in phosphate chains of moderate length. The last significant contribution (at about −15 ppm) is attributed to the $[P_2O_7]^{4-}$ diphosphate groups. This spectrum thus indicates a chain length distribution in the glass network. It is important to remark the splitting of the Q_2-Q_2 autocorrelation peak along the diagonal of the spectrum. This splitting indicates that the Q_2-Q_2 dipolar interaction involves two structurally different Q_2 sites having distinct isotropic chemical shifts (the average chemical shift difference between two coupled Q_2 nuclei is about 2.5 ppm).

As shown in Figure 6c, the Q_2-Q_2 and Q_2-Q_1 correlation peaks are clearly resolved in the double-quantum spectrum of the glass containing 55 mol % PbO. In this case, the remaining very weak Q_1-Q_1 contribution is attributed to long-range dipolar couplings.

The double-quantum spectrum of the metaphosphate glass (Figure 6d) exhibits a single intense autocorrelation peak revealing Q_2-Q_2 connectivities. The structural motifs consistent with the spectrum are linear (or cyclic) long phosphate chains as those involved in the $Pb(PO_3)_2$ crystalline structure. In analogy with the two previous samples, we observe a splitting of the Q_2-Q_2 autocorrelation peak along the diagonal.

We mentioned above that the isotropic chemical shift and the line width of the Q_n units depend on glass composition and thus glass network structure. From the double-quantum experiments, we also remark that the auto (Q_n-Q_n) and cross-correlation (Q_n-Q_m) peaks are located at different isotropic positions in the single quantum dimension. This suggests that the Q_n isotropic chemical shift is directly influenced by the type of the linked adjacent Q_n unit. A similar trend has recently been observed in the double-quantum spectra of $Na_2O-P_2O_5$[17] and $CaO-P_2O_5$[18] glasses. The Q_n species can be thus classified according to their connectivities, $Q_{n,ij}$, where the additional subscripts describe the type of the bonded PO_4 group.[18] As described above, the Q_n line widths and chemical shift ranges increase with the number of bridging oxygen atoms per Q_n units. It should be pointed out that, in a similar way, the number of the possible local configurations around the Q_n species increases with its number of bridging oxygen atoms: a Q_1 group can be bound to a Q_1 ($Q_{1,1}$) or a Q_2 unit ($Q_{1,2}$), while a Q_2 group can form $Q_{2,11}$, $Q_{2,12}$, $Q_{2,22}$, $Q_{2,23}$, or $Q_{2,33}$ species. The $Q_{n,ij}$ isotropic shifts and line widths, reported in Table 3, were determined from the positions of the auto and cross-correlation peaks in the single quantum dimension. We observe that changing the nature of the neighboring Q_n unit results in an average shift of about 2 ppm for both $Q_{1,i}$ and $Q_{2,ij}$ species. The $Q_{n,ij}$ line widths indicate a strong overlap of their respective chemical shift ranges, in agreement with the results obtained for the crystalline compounds: the $Q_{1,1}$ isotropic shifts, measured for $Pb_2P_2O_7$, lies between −8.4 and −12 ppm while the $Q_{1,2}$ sites found in $Pb_3P_4O_{13}$ lead to resonances at −9.9 and −10.8 ppm.

Since the excitation of double-quantum coherence can hardly be quantitative, the determination of the relative $Q_{n,ij}$ concentra-

(34) Brow, R. K.; Kirkpatrick, R. J.; Turner, G. L. *J. Non-Cryst. Solids* **1990**, *116*, 39−45.
(35) Losso, P.; Schnabel, B.; Jäger, C.; Sternberg, U.; Stachel, D.; Smith, D. O. *J. Non-Cryst. Solids* **1992**, *143*, 265−273.
(36) Mason, J. *Solid State NMR* **1993**, *2*, 285−288.

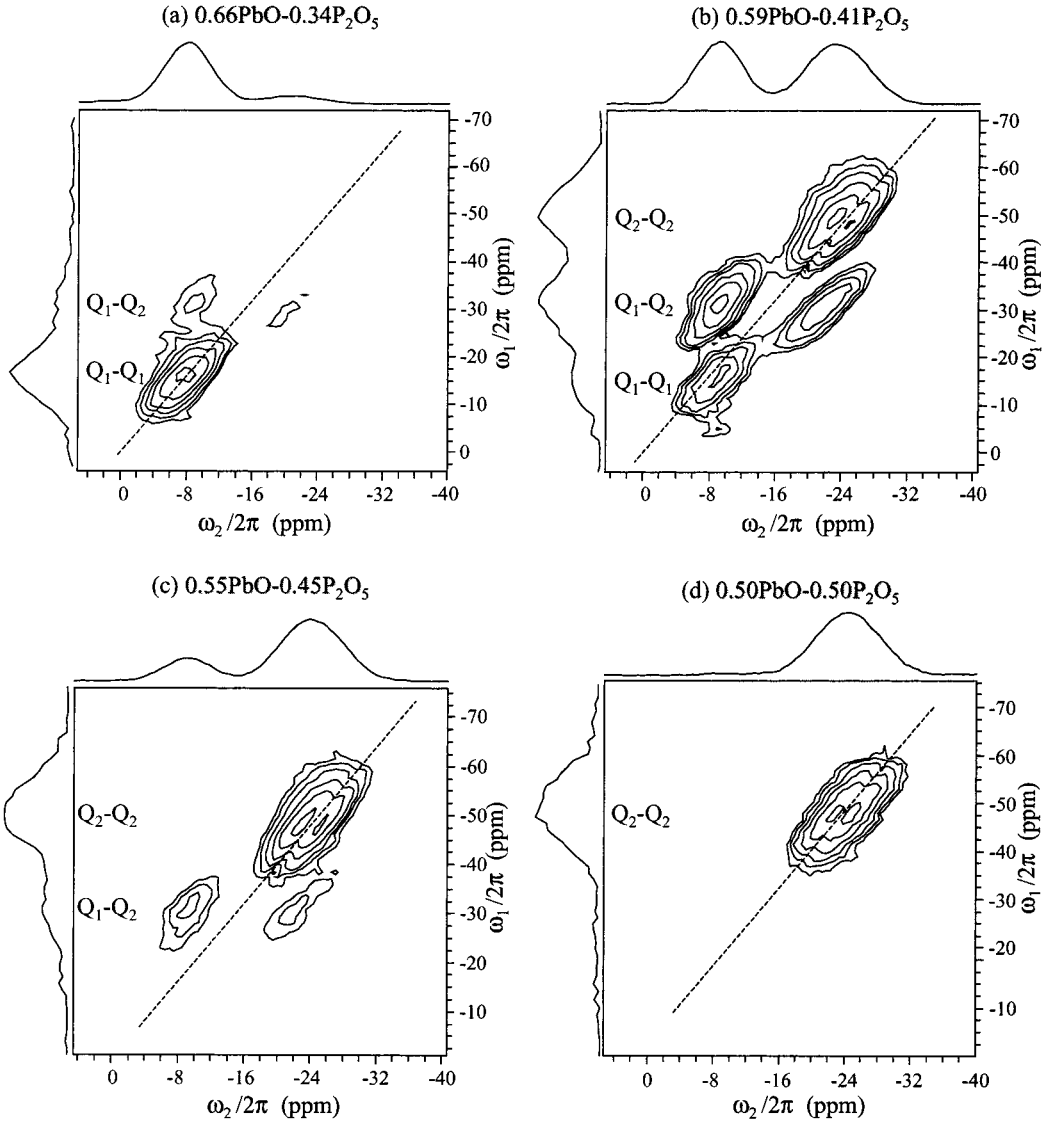

Figure 6. ^{31}P double-quantum MAS spectra of the glasses $0.66PbO-0.34P_2O_5$ (a), $0.59PbO-0.41P_2O_5$ (b), $0.55PbO-0.45P_2O_5$ (c), and $0.50PbO-0.50P_2O_5$ (d). The contour levels were set to 16.7, 23.4, 32.8, 45.9, 64.2, and 90% of the maximal peak intensity.

tions from double-quantum spectra is not straightforward. Nevertheless, it is possible to determine these concentrations from the simulations of the quantitative 1D MAS spectra using the parameters obtained from 2D spectra and constraining the $Q_{n,ij}$ positions and line widths to vary within a range of ± 0.5 ppm. Moreover, the stoechiometry of the system imposes another constraint that is $[Q_{1,2}] = 2[Q_{2,11}] + [Q_{2,21}]$. Following this protocol, we have estimated the relative populations of $Q_{n,ij}$ units given in Table 3. These relative $Q_{n,ij}$ populations are in good agreement with the previous quantification of Q_n species. For PbO content higher than 55 mol %, the phosphate network is composed of Q_2, Q_1, and Q_0 species. For this compositional range, only the Q_2 and Q_1 species have P−O bridging bonds. Thus, assuming a homogeneous distribution of Q_2 and Q_1 units in the glass, a random phosphorus connectivity scheme can be described using a binomial distribution of Q_2 and Q_1 bridging bonds as proposed by Alam and Brow.[16] As shown in Figure 7, the experimentally determined $Q_{n,ij}$ populations are consistent with those calculated from the Q_n populations assuming a binomial distribution of connectivities in the glass structure. It should also be pointed out that for the glasses with high lead content, the phosphate chain-length distribution can be deduced from these $Q_{n,ij}$ concentrations, as discussed by Witter et al..[18]

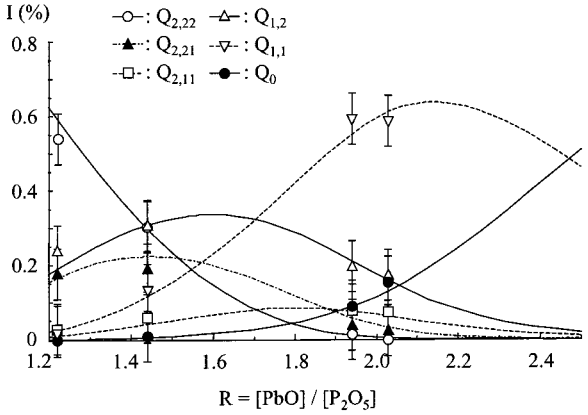

Figure 7. Experimentally determined $Q_{n,ij}$ distributions in lead phosphate glasses as a function of the $[PbO]/[P_2O_5]$ ratio. The fitted lines were calculated from the Q_n populations assuming a binomial distribution of connectivities in the phosphate network.

These results show that the high-resolution double-quantum NMR experiment can be used to improve the structural description of the phosphate network and to obtain intermediate range order information in phosphate based glasses.

Conclusion

Using solid-state ^{31}P MAS and 2D double-quantum NMR, we have investigated the local and intermediate range ordering around phosphorus in binary $PbO-P_2O_5$ glasses. The distribution of the Q_n species, determined from the simulation of 1D MAS spectra, indicates a significant disproportionation reaction ($2Q_n \leftrightarrow Q_{n+1} + Q_{n-1}$) near the pyrophosphate composition, which is attributed to the appearance of more covalent Pb−O bonds in the glass structure. As shown in the case of crystalline reference samples, the connectivities between Q_n groups can be determined from 2D double-quantum spectra. This allowed us to probe the phosphorus connectivity scheme in the glass network and to show that the Q_n chemical shift is directly influenced by the type of the adjacent PO_4 tetrahdron ($Q_{n,ij}$ species). By simulating the quantitative 1D MAS spectra using $Q_{n,ij}$ chemical shifts obtained from double-quantum spectra, the relative $Q_{n,ij}$ concentrations and their evolutions with the glass composition have been estimated.

Acknowledgment. This work was supported by CNRS (UPR 4212) and Région Centre. The authors thank C. Jäger for useful discussion.

IC990375P